Stick-slip dynamics, Extreme value statistics & avalanches in moving contact lines and solid friction

Caishan Yan, Hsuan-Yi Chen, Pik-Yin Lai (黎璧賢), Penger Tong
Dept. of Physics & Center for Complex Systems, National Central Univ., Taiwan
Physics, Division, National Center for Theoretical Sciences, Taipei, Taiwan
Email: pylai@phy.ncu.edu.tw

DDAP13 Kyoto, July 2024

- Introduction
- Stick-slip dynamics of a mesoscale moving contact line
- Stick-slip motion of dry friction at mesoscale
- Modified Prandtl and Tomlinson (PT) model

- “Statistical laws of stick-slip friction at mesoscale”, Nature Comm. **14**:6221 (2023).
- “Avalanches and extreme value statistics of a mesoscale moving contact line, PRL **132**, 084003 (2024) (Editor’s suggestion)

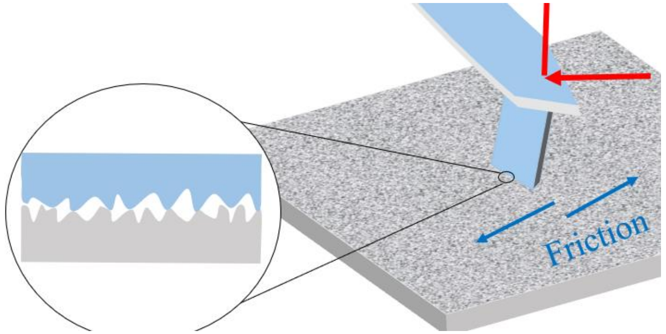

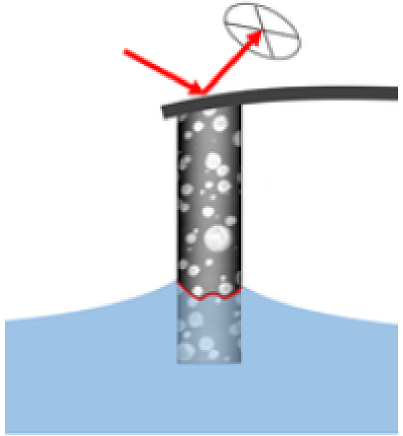

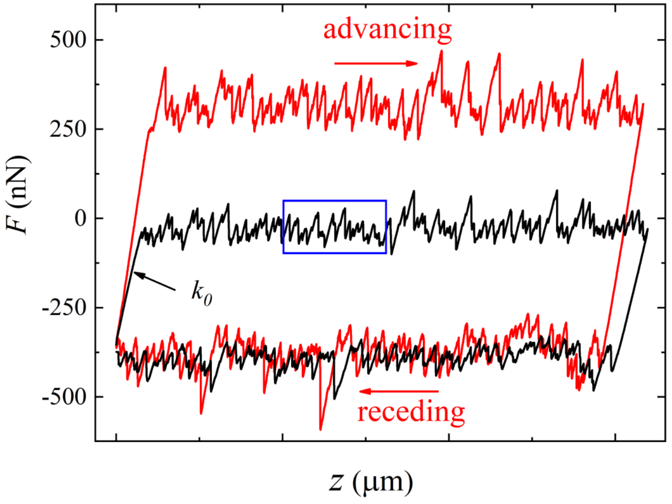

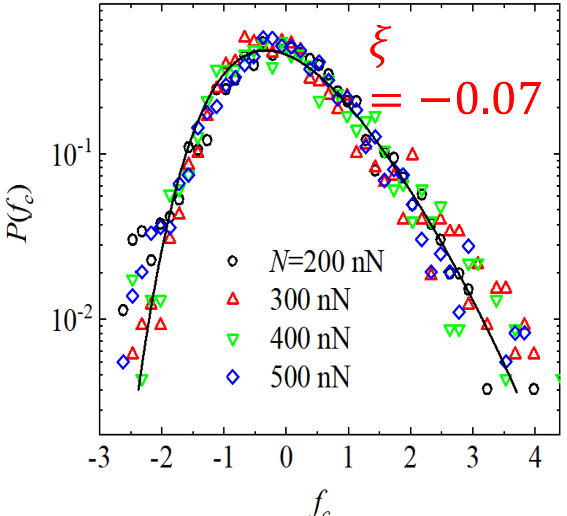

Stick-slip and avalanche dynamics

- Stick-slip is a class of phenomena characterized by intermittent jerky movement in out-of-equilibrium disordered systems, as a yield response to a smoothly-varying external force.

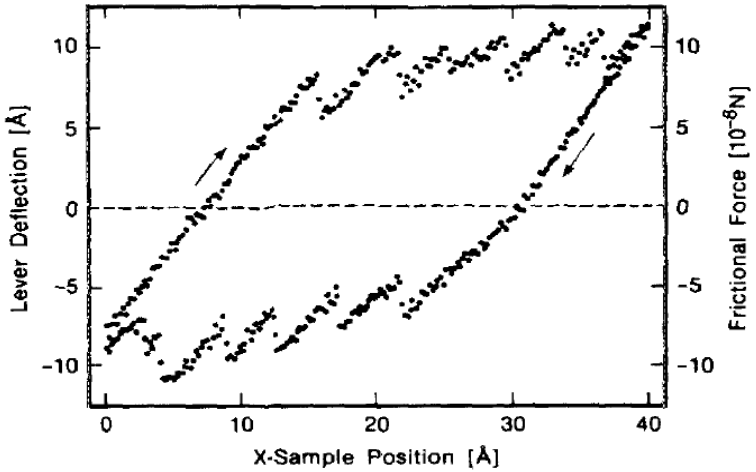

Erlandsson *et al.* (1988)

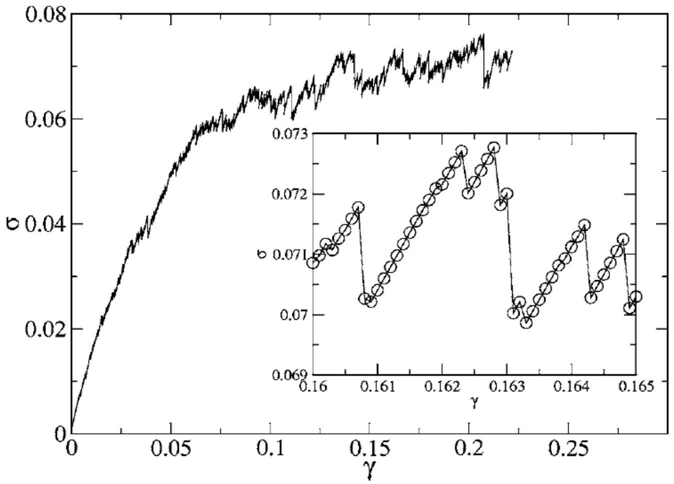

Maloney & Lemaitre (2006)

- It is observed in nature and many engineering applications that span a wide range of scales, from the nanoscale contacts and fractures in nano- and micro-machines/devices to the geophysical scale of snow avalanches, landslides and earthquakes.

- Rapture of single molecules (zero-dimension)
- Pinning and depinning of a three-phase contact line and vortex lines in type-II superconductors (one-dimension)
- Friction between two solid surfaces and dynamics of ferromagnetic domain walls (two-dimension)
- Plasticity of amorphous solids under a simple shear (three-dimension)

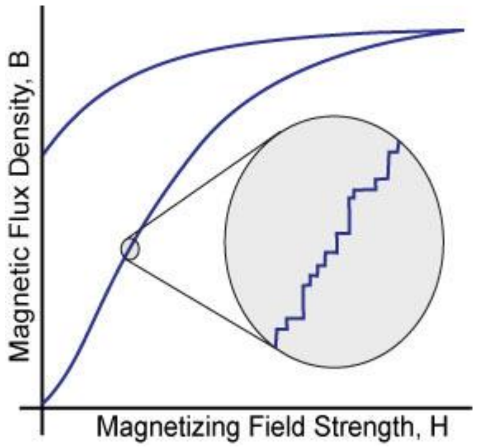

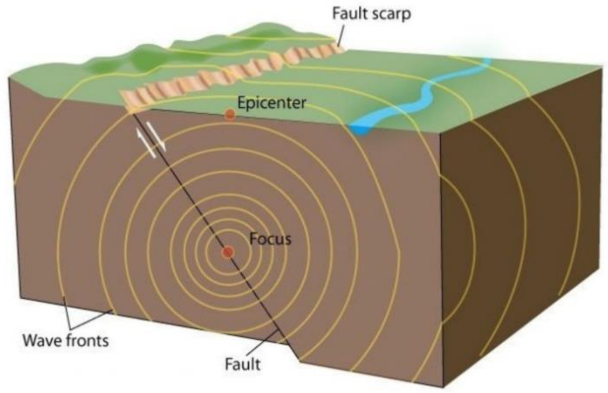

- A common feature of stick-slip events is their broad range of slip lengths, manifest as power-law distributions of many orders of magnitude. The fact that very different systems behave in a similar manner has prompted extensive investigations for a common mechanism underpinning these phenomena.

- There are a number models and proposals aimed at explaining the power-law distributions, but many of them have not been confirmed by experiment. Theory and experiment do not converge, because the out-of-equilibrium systems involved are often disordered, and disorder has many different forms.

pinning-depinning of a three-phase contact line

For an idealized surface (atomically smooth, chemically homogenous & infinitely hard) at equilibrium:

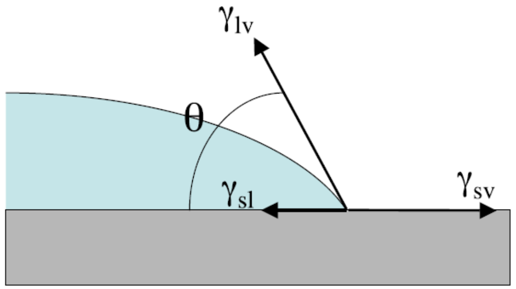

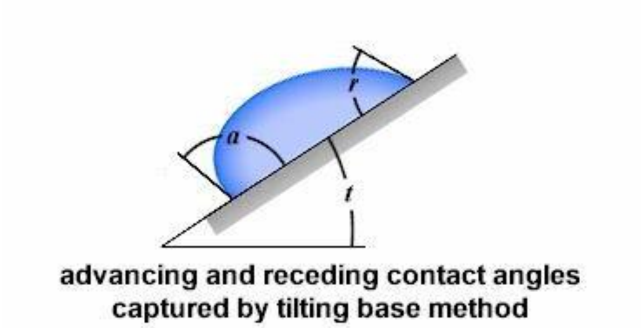

Young's equation:

$$\gamma_{lv} \cos\theta = \gamma_{sv} - \gamma_{sl}$$

Hysteresis: $\theta_a > \theta_r$

$$f_h = \gamma_{lv}(\cos\theta_r - \cos\theta_a)$$

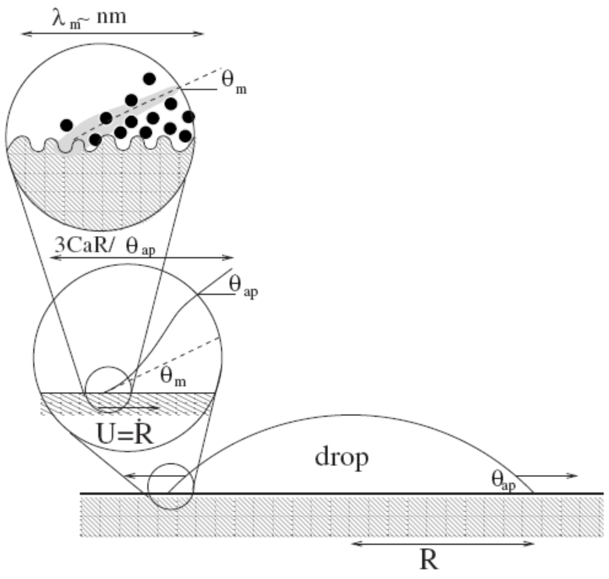

- **Contact angle hysteresis (or capillary force hysteresis)** is caused by the pinning of the contact line by physical roughness or chemical heterogeneity on the solid surface ($\delta x = (k_B T/\gamma)^{1/2} \approx 0.2$ nm).
- For mesoscale systems, one finds large amplitude fluctuations of the capillary force, in addition to its mean value change f_h.
- How contact angle hysteresis is determined by the underlying pinning force field?

Stick-slip dynamics of a moving contact line at mesoscales:

small enough to resolve the slip events at the single slip resolution but is also large enough to allow the individual slips to have a broad range of slip sizes in a well-characterized defect landscape

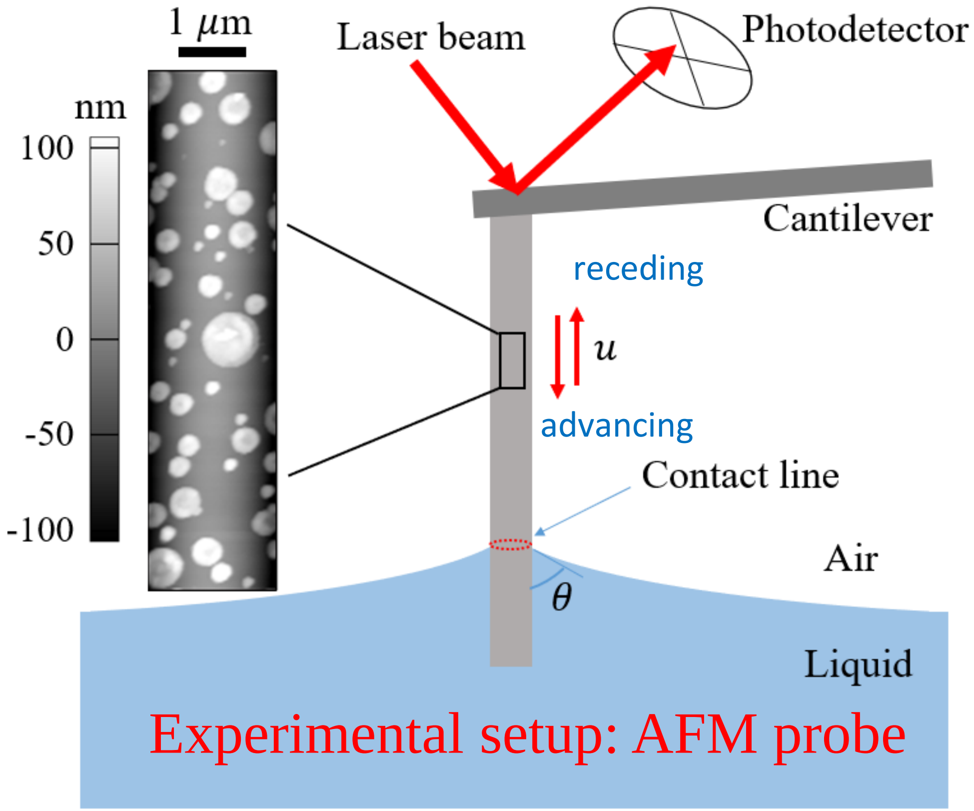

Experimental setup: AFM probe

Surface coating: propyl trichlorosilane (PTS)

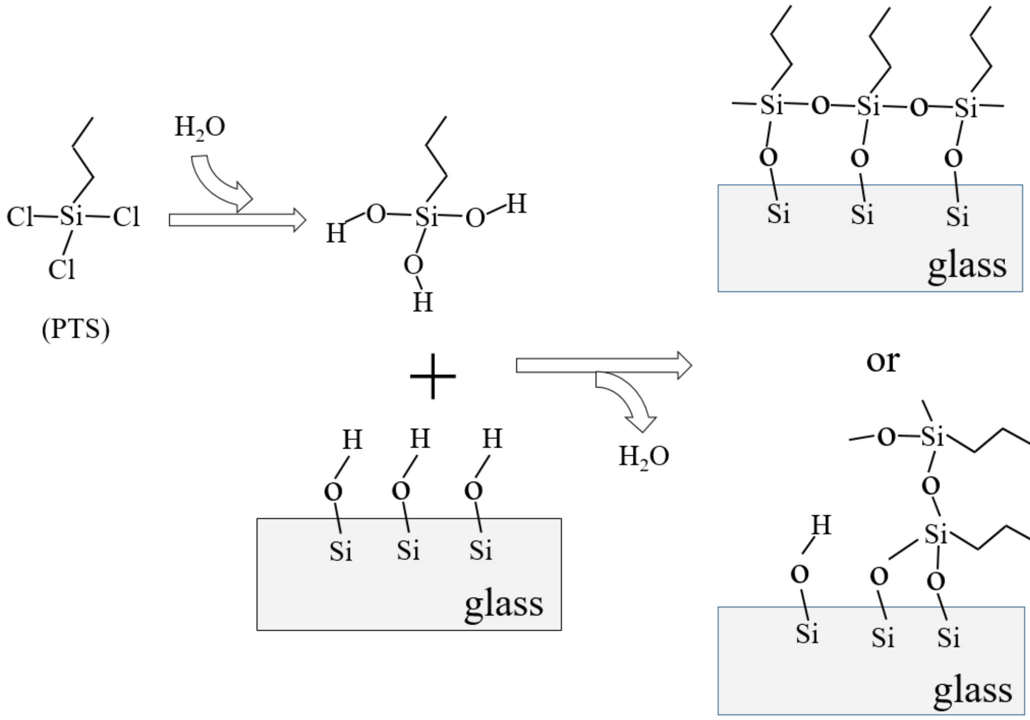

- Long glass fiber diameter *d*: 0.4-4 μm, at mesoscale to resolve single slip events
- fiber length *L*: 100-300 μm
- Low-speed limit: u~0.62 μm /s (viscous drag is negligible)

Stick-slip dynamics of a moving contact line

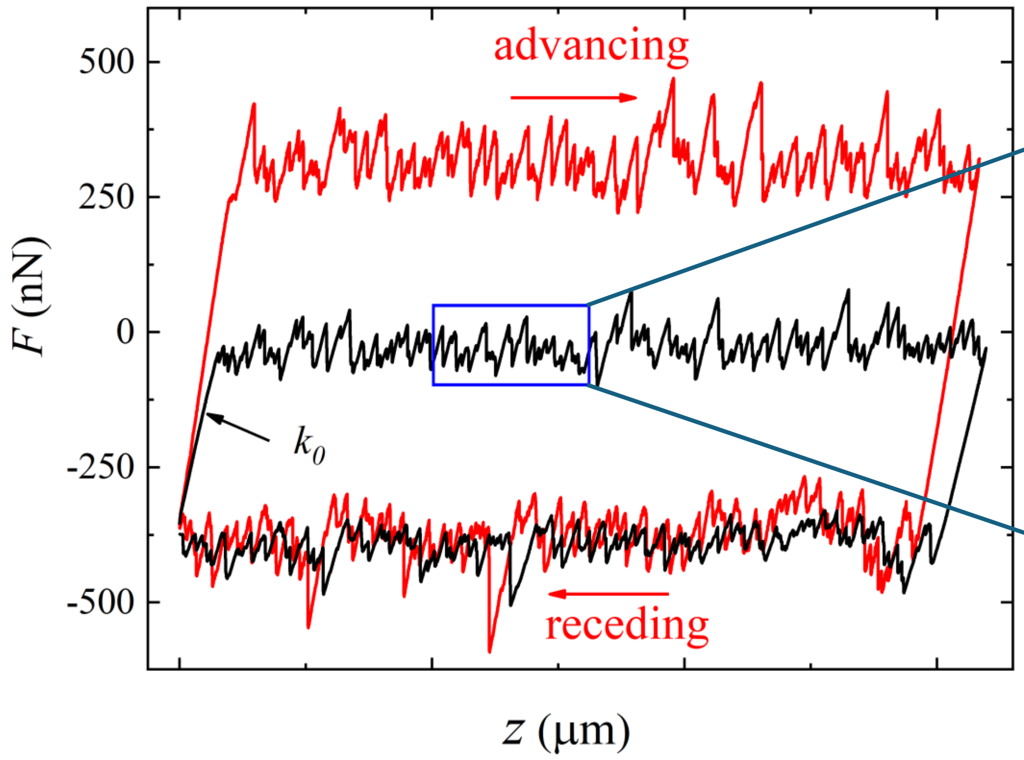

Fluctuating stick-slip dynamics:

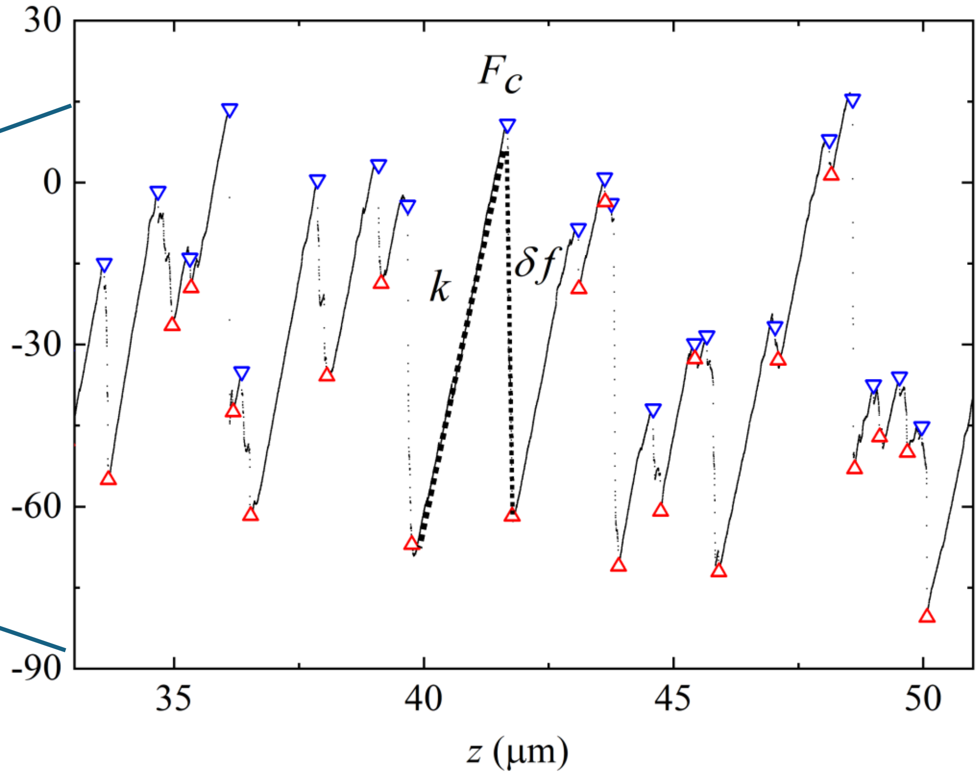

Capillary force hysteresis loop for water (red) and ethylene glycol (black)

Static spring constant of the liquid interface, $k_0 \sim \gamma$

F_c: critical depinning force (onset of slip)

δf: force release during the slip

k: dynamics spring constant of interface (linear force accumulation)

Stick-slip dynamics of friction between 2 solid surfaces

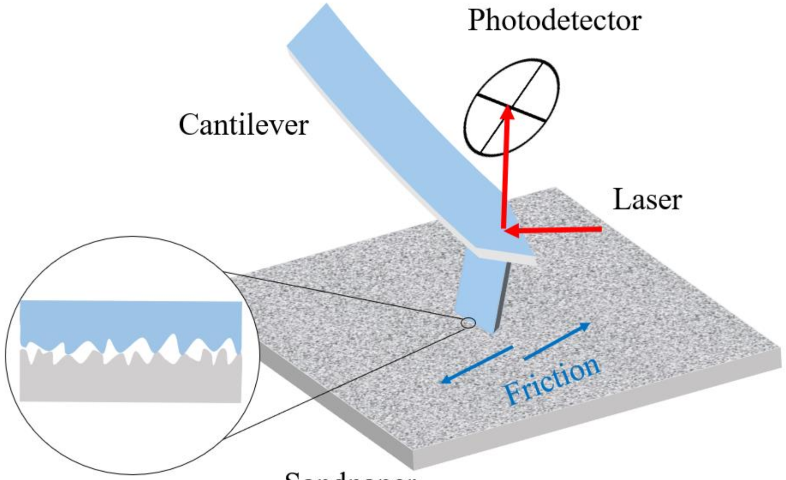

Lateral hanging-beam AFM

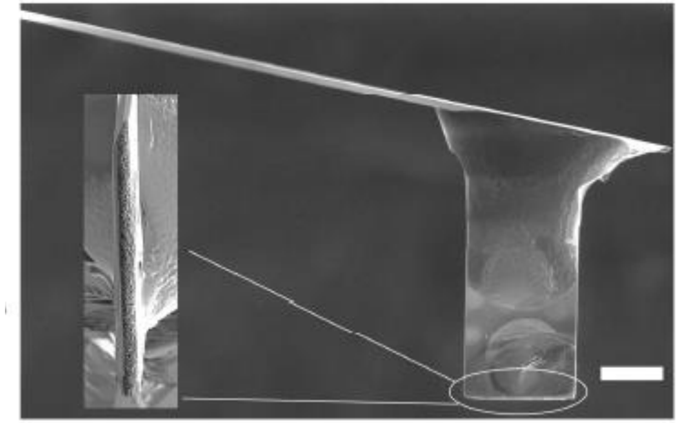

Quasi-1D scanning probe with an end contact area of 34×3 μm² (UV glue)

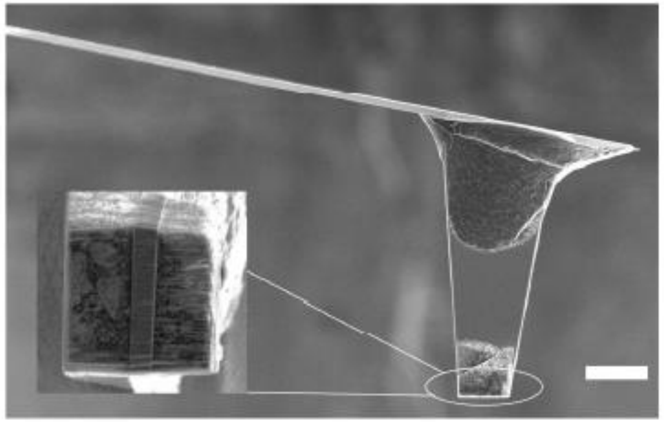

2D scanning probe with an end contact area of 12×12 μm²(UV glue).

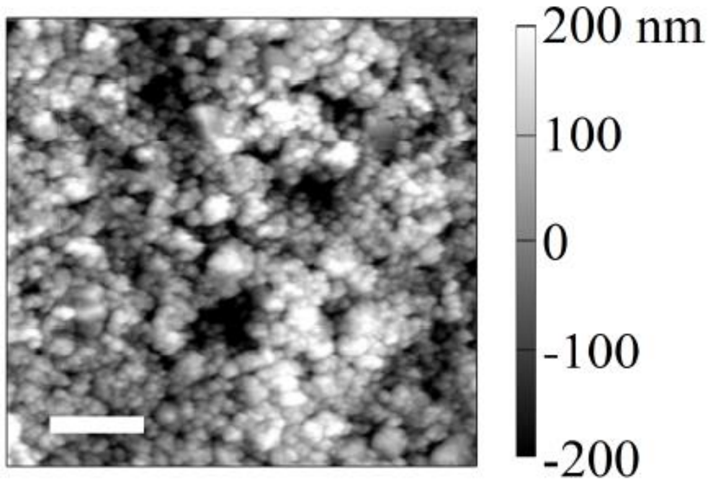

Ultra-fine sandpaper (silicon carbide) surface with an average grain size 0.1 μm

Evolution of contact geometry with increasing normal load N

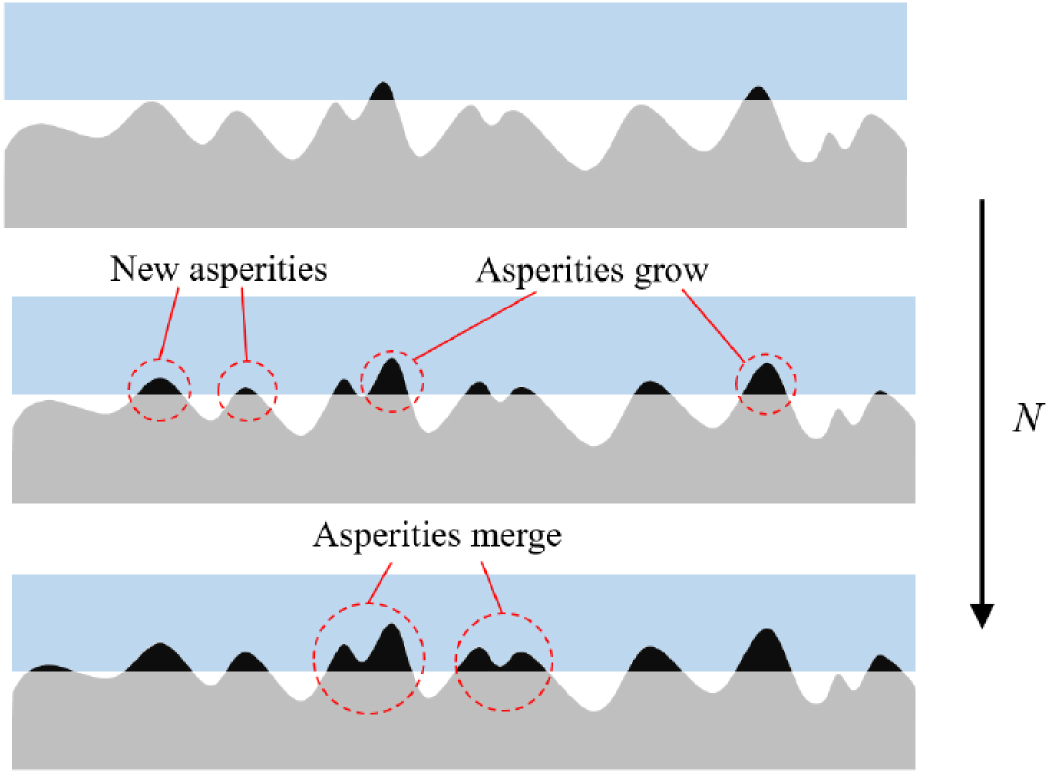

- In the low-load regime, the asperities (or microcontacts) at the interface are dilute, and their number increases with the normal load *N*.
- In the high-load regime, coalescence between nearby asperities occurs.
- In the intermediate range of *N* (200–600 nN), an "optimal contact" between the scanning probe and sandpaper is achieved, with the number of the asperities is kept at ~O(100) for a mesoscale scanning probe.

Stick-slip dynamics of friction between 2 solid surfaces

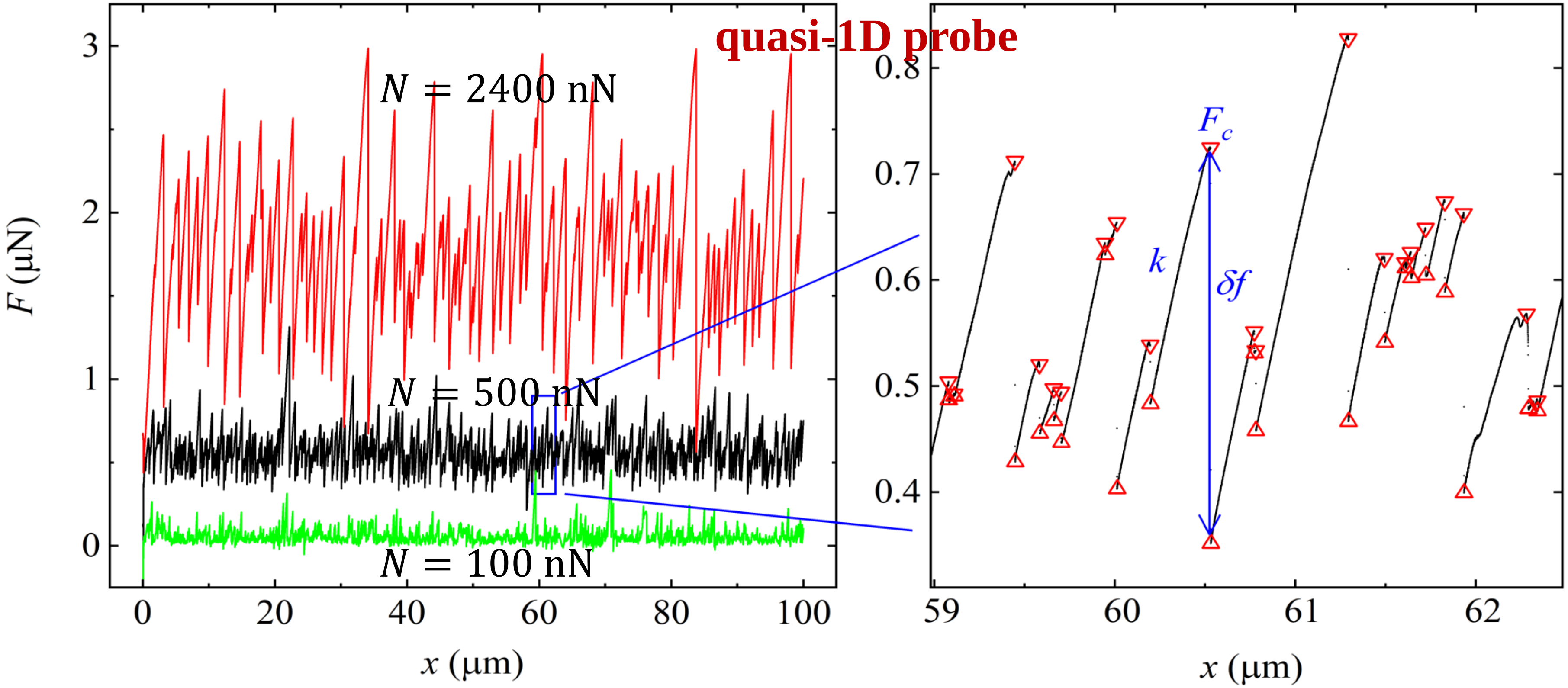

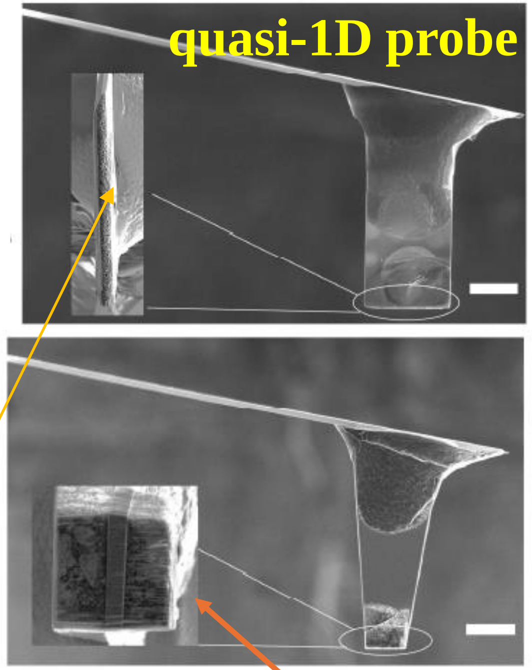

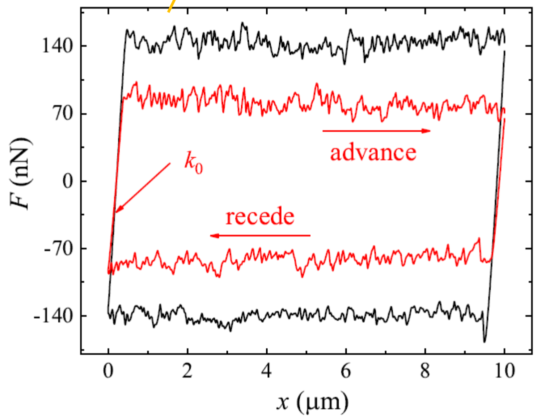

2D probe

- Increasing normal load N: smooth sliding → stick-slip

- focus on the intermediate range of normal load (200–600 nN) at an “optimal contact” with the sandpaper so that it can sense the full range of the rough landscape with negligible wear

k, F_c, and δf reveal universal statistical properties for dry friction & CL

Distribution of the stick-slip events: Depinning force $f_c = \frac{F_c - \langle F_c \rangle}{\sigma_{F_c}}$

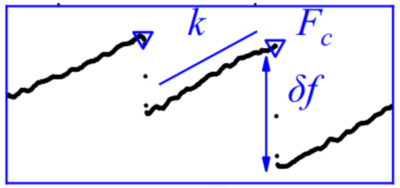

Contact line

water, 66 wt.% glycerol aqueous solution, and ethylene glycol

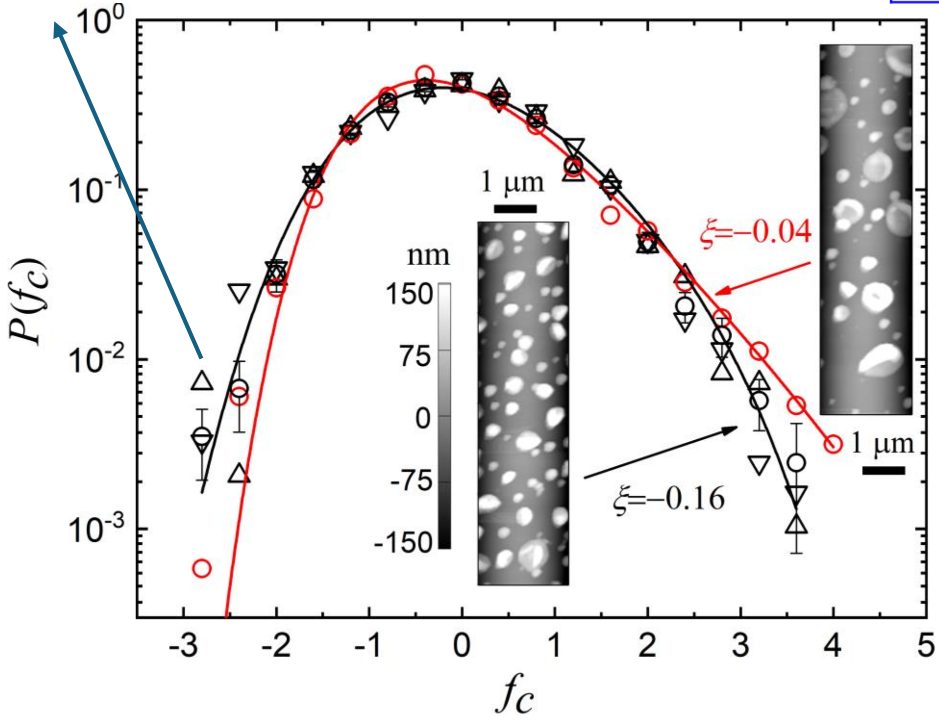

Solid friction

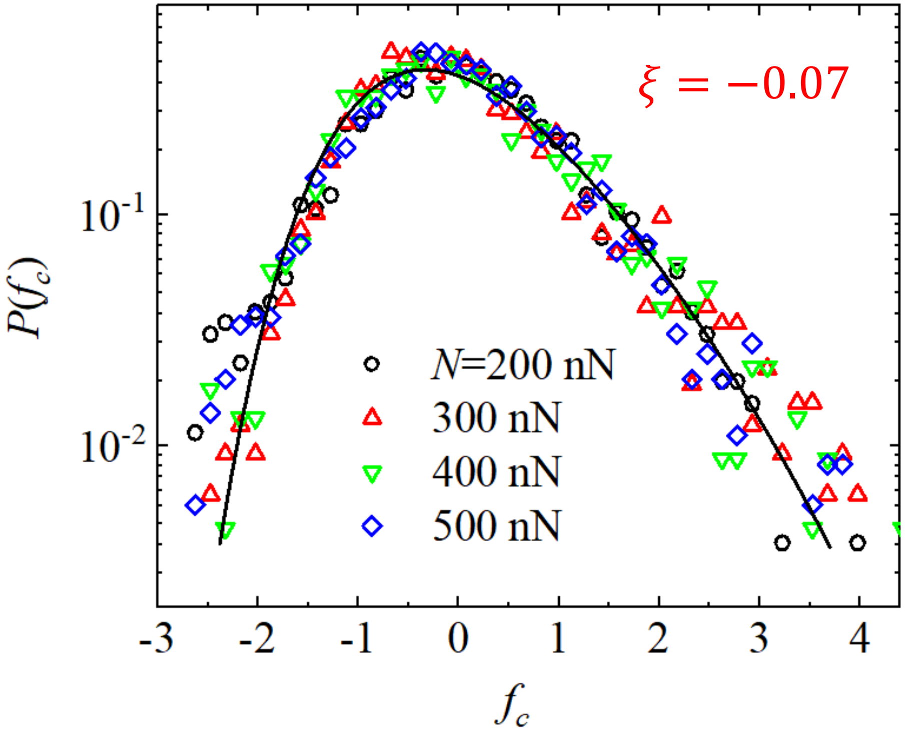

Generalized-extreme-value (GEV) distribution:

$$p(f_c) = \frac{1}{\beta}\left(1 + \xi\,\frac{f_c - \mu}{\beta}\right)^{-1/\xi} \exp\left[-\left(1 + \xi\,\frac{f_c - \mu}{\beta}\right)^{-\frac{1}{\xi}}\right],$$

$$\left(\begin{array}{c} \mu = \beta(1 - \Gamma(1 - \xi))/\xi \\ \beta = \xi/\sqrt{\Gamma(1 - 2\xi) - \Gamma^2(1 - \xi)} \end{array}\right)$$

Generalized Extreme Value (GEV) distribution

- GEV models the distribution of extreme values in a dataset. Commonly used in environmental science, economics, and engineering to analyze events such as extreme weather conditions or financial market crashes.
- Help to understand how likely the extreme(the highest or lowest) values are to occur.
- Examples: predicting the maximum wind speed in a particular location, estimating the size of the worst floods in a river, or analyzing the extreme values of stock market returns during a financial crisis.

Statistics or distribution of the maximum (or minimum) of n (a large number) samples drawn independently from an identical probability distribution.

Extreme-value Theorem: the random variable $x=max\{X_i\}^n_{i=1}$ follows one of the **generalized extreme value** (**GEV**) **distributions** (the Gumbel, Fréchet and Weibull families also known as type I, II and III extreme value distributions)

$$\mathrm{GEV}(\mu, \sigma, \xi) = \frac{1}{\sigma} t(x)^{\xi+1} e^{-t(x)},$$

where

$$t(x) = \begin{cases} \left(1+\xi\left(\frac{x-\mu}{\sigma}\right)\right)^{-1/\xi} & \text{if } \xi \neq 0 \\ e^{-(x-\mu)/\sigma} & \text{if } \xi = 0 \end{cases}$$

$\xi \approx 0$

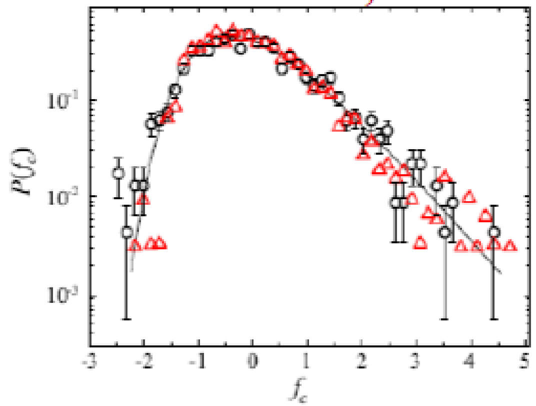

Extreme value Theorem: three types of GEV distributions

$$\mathrm{GEV}(\mu,\,\sigma,\,\xi) = \frac{1}{\sigma}\,t(x)^{\xi+1}e^{-t(x)},$$

where

$$t(x) = \begin{cases} \left(1+\xi\left(\frac{x-\mu}{\sigma}\right)\right)^{-1/\xi} & \text{if } \xi \neq 0 \\ e^{-(x-\mu)/\sigma} & \text{if } \xi = 0 \end{cases}$$

- Gumbel or type I extreme value distribution ($\xi = 0$)

$$F(x;\mu,\sigma,0) = e^{-e^{-(x-\mu)/\sigma}} \quad \text{for } x \in \mathbb{R}.$$

Cumulation distribution

$$\boxed{\text{Pdf: } p(x) = \frac{1}{\sigma}\,e^{-(z+e^{-z})} \text{ where } z = \frac{x-\mu}{\sigma}}$$

- Fréchet or type II extreme value distribution, if $\xi = \alpha^{-1} > 0$ and $y = 1 + \xi(x-\mu)/\sigma$

$$F(x;\mu,\sigma,\xi) = \begin{cases} e^{-y^{-\alpha}} & y > 0 \\ 0 & y \leq 0. \end{cases}$$

- Reversed Weibull or type III extreme value distribution, if $\xi = -\alpha^{-1} < 0$ and $y = -(1 + \xi(x-\mu)/\sigma)$

$$F(x;\mu,\sigma,\xi) = \begin{cases} e^{-(-y)^{\alpha}} & y < 0 \\ 1 & y \geq 0 \end{cases}$$

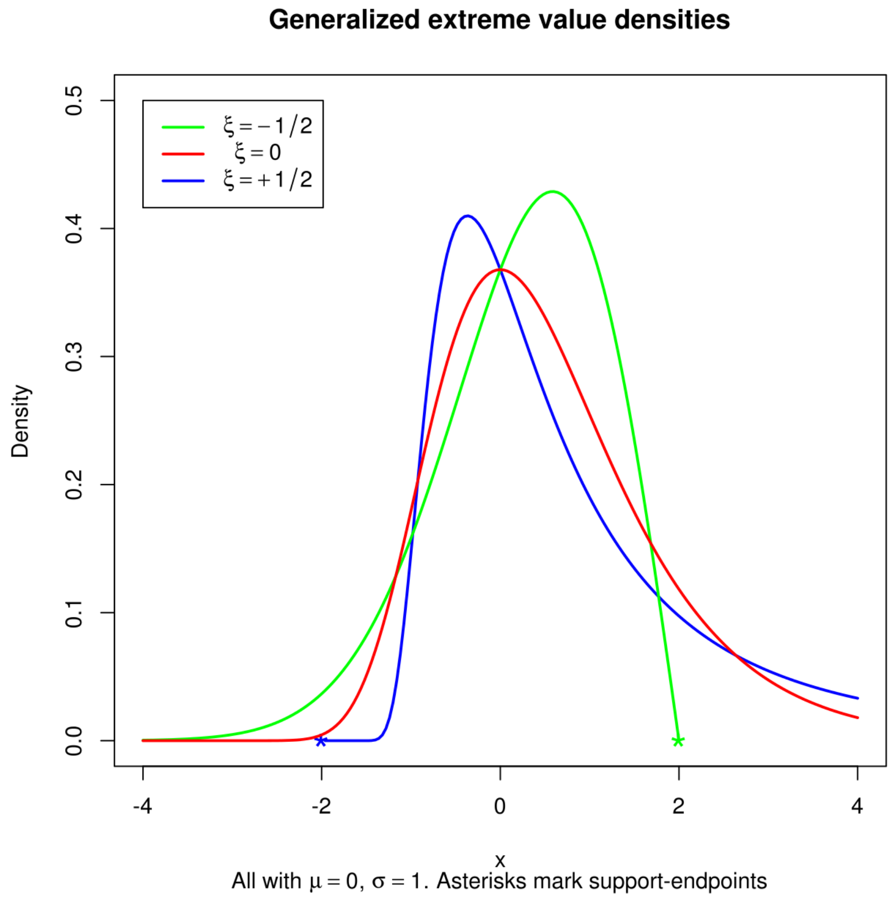

Examples of Extreme Value Statistics:

Characteristic time scales near the laminar-turbulent transition in the pipe flow

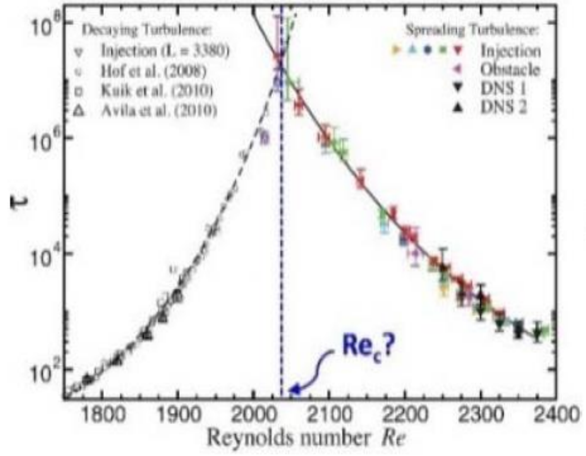

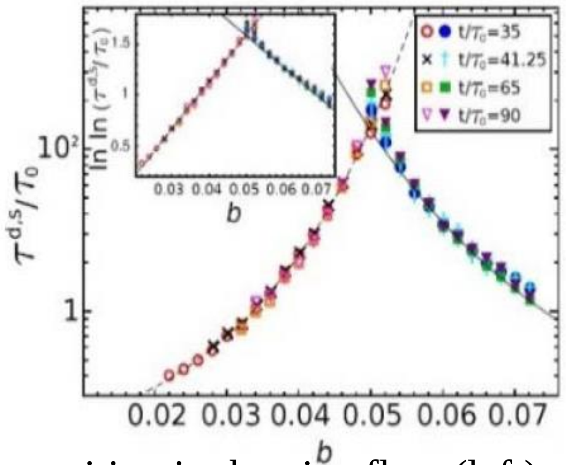

Avila et. al Science 333, 192 (2011)
HY Shih et. al, Nat. Phys. **12**, 245,(2018)

Super-exponential in τ is related to Gumbel distribution: Active state persists until the ***most*** long-lived percolating strand decays

Characteristic time scales near the laminar-turbulent transition in the pipe flow (left) and the scaling near predator extinction in the predator-prey model (right). The mean decay and splitting times of the turbulent density and the prey density scale with Reynolds number

Large-scale circulations in turbulent thermal convection: the plume eruption amplitude follows the GEV distributions

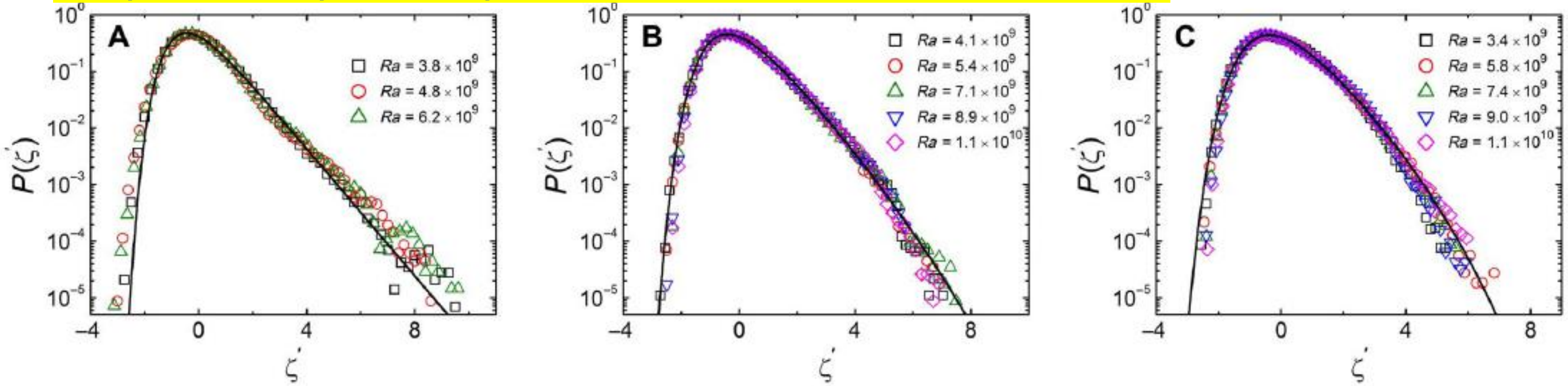

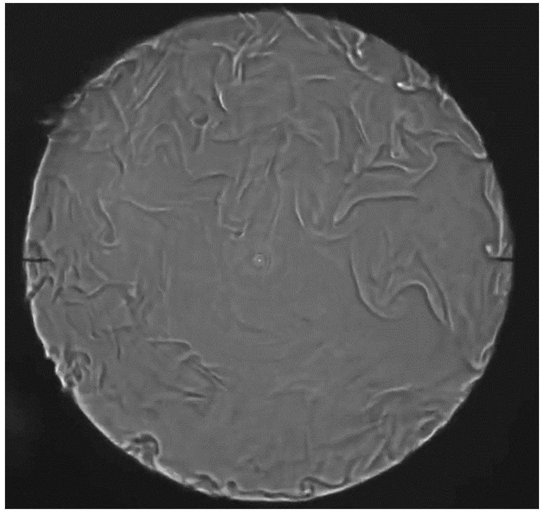

Fig. 3. *Ra* dependence of the PDF of the massive eruption events. (A to C) Measured PDF $P(\zeta')$ (open symbols) as a function of the normalized variable $\zeta'=\zeta/\sigma_\zeta$ with different values of *Ra* for (A) water (*Pr* = 4.4), (B) 10% glycerin solution (*Pr* = 5.7), and (C) 20% glycerin solution (*Pr* = 7.6). The solid lines show the fits of the GEV distribution in Eq. 3 to the data points with (A) χ = −0.001, (B) χ = −0.04, and (C) χ = −0.07, respectively.

Y. Wang et. al., Sci. Adv. 4: eaat7480 (2018)

Extreme Value Statistics in moving contact line: contact line deforms and eventually depinning occurs

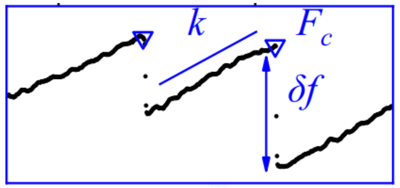

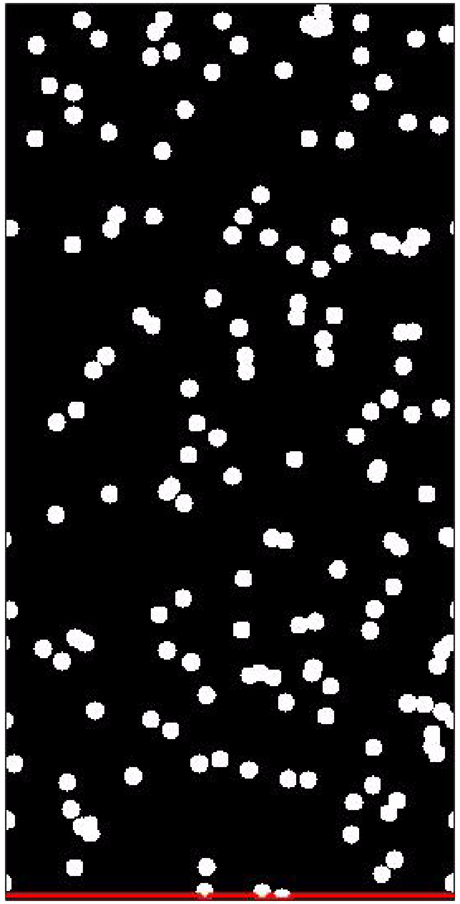

- contact line deforms to accumulate stronger force to de-pin
- A large number of pinning sites along the contact line loop
- Fc ~ maximum of the pinning forces
- As the contact line is pulled: sample the maximum of the (~independent pinning forces) on the contact line → GEV

Normalized depinning force $f_c = \frac{F_c - \langle F_c \rangle}{\sigma_{F_c}}$

F_c contains an eqm. force $F_{eq} = -\pi d \gamma \cos\theta$

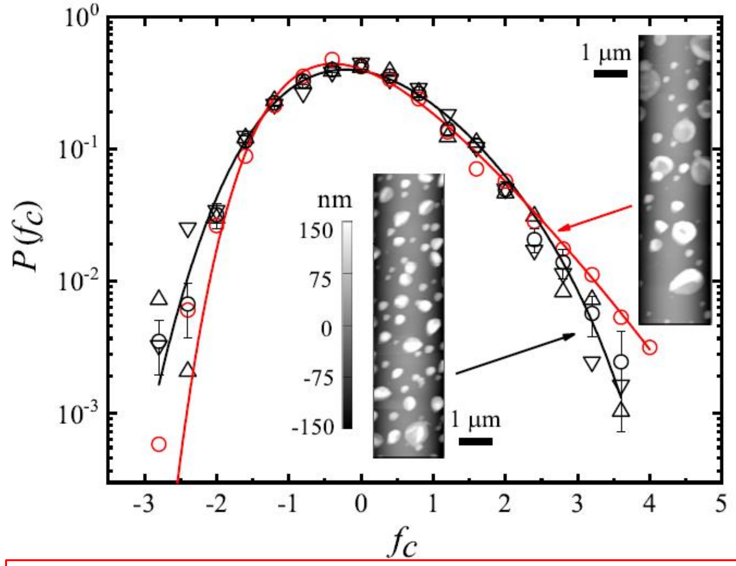

$$P(f_c) = \frac{1}{\beta}(1+\xi z)^{-(1+1/\xi)} e^{-(1+\xi z)^{-1/\xi}}$$

ξ = -0.17 (black line) ξ = -0.06 (red line)

ξ < 0 reversed Weibull distribution: has an upper bound $(f_c)_M = \mu - \beta/\xi$ beyond which $P(f_c) = 0$ → an upper bound for $(F_c)_M$. Roughness-induced maximal pinning force = $(F_c)_M - F_{eq}$, larger for the rougher surface(750 vs. 402 nN)

ξ = 0 Gumbel distribution: exponential tail with an infinite upper bound $[(f_c)_M \rightarrow \infty]$.

Distribution of the stick-slip events for the contact line:

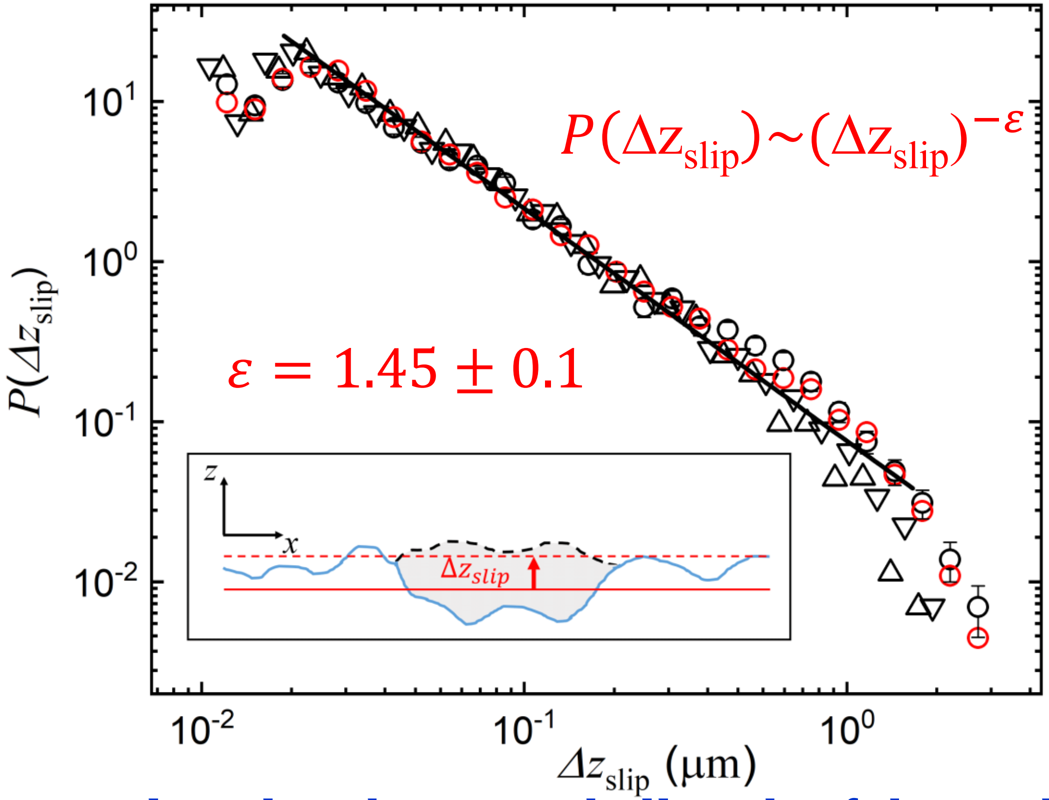

slip length $\Delta z_{\text{slip}} = \frac{\delta f}{k_0}$

Static spring constant of the liquid interface, k_0

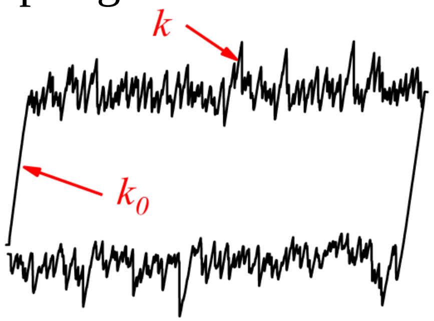

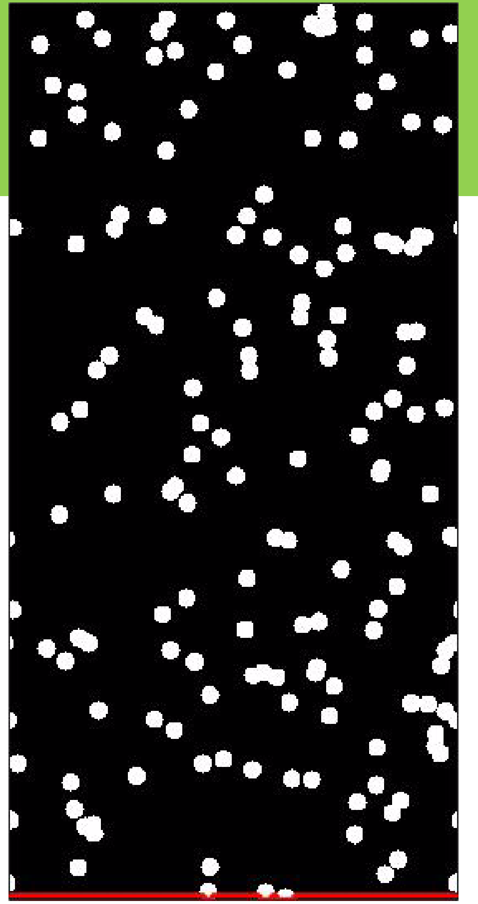

- Power-law distribution is hallmark of the avalanche dynamics.
- when a strong defect slips, the released large stress is partially transferred to its neighboring defects and triggers their slips→ avalanche
- ϵ is unchanged for fibers with different roughnesses and in contact with different liquids
- In the low-speed limit, the Alessandro-Beatrice-Bertotti-Montorsi(ABBM) model predicts ϵ =3/2 → slow CL motion obeys the ABBM model

Distribution of the stick-slip events: Slip length= $\frac{\delta f}{k_0}$

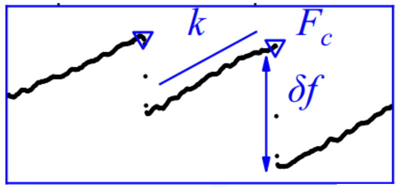

Contact line

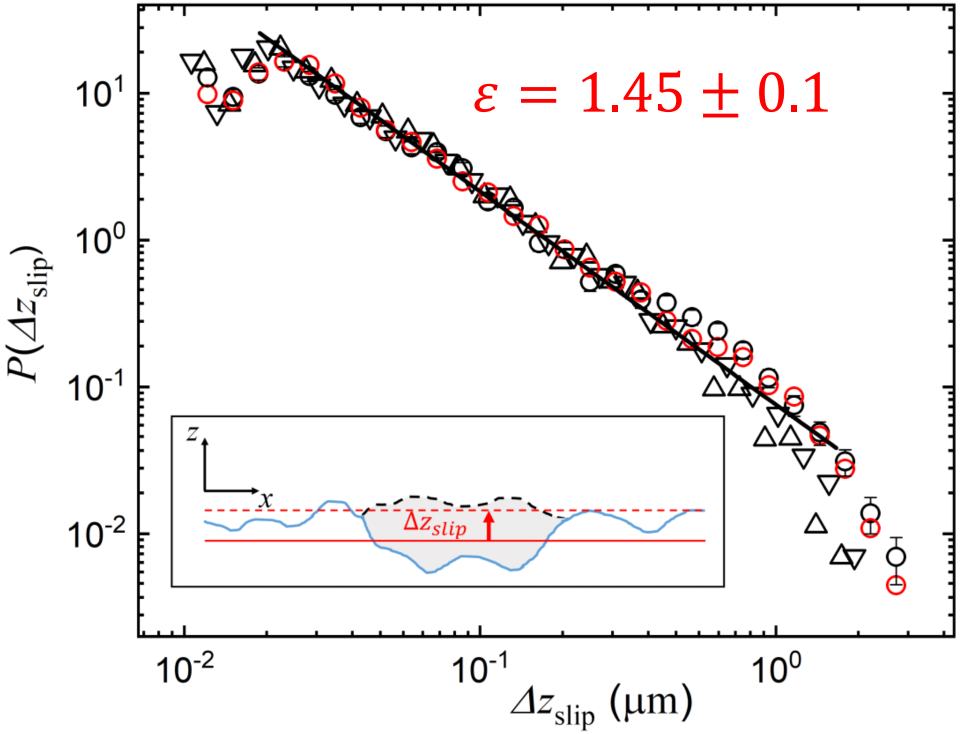

Solid friction

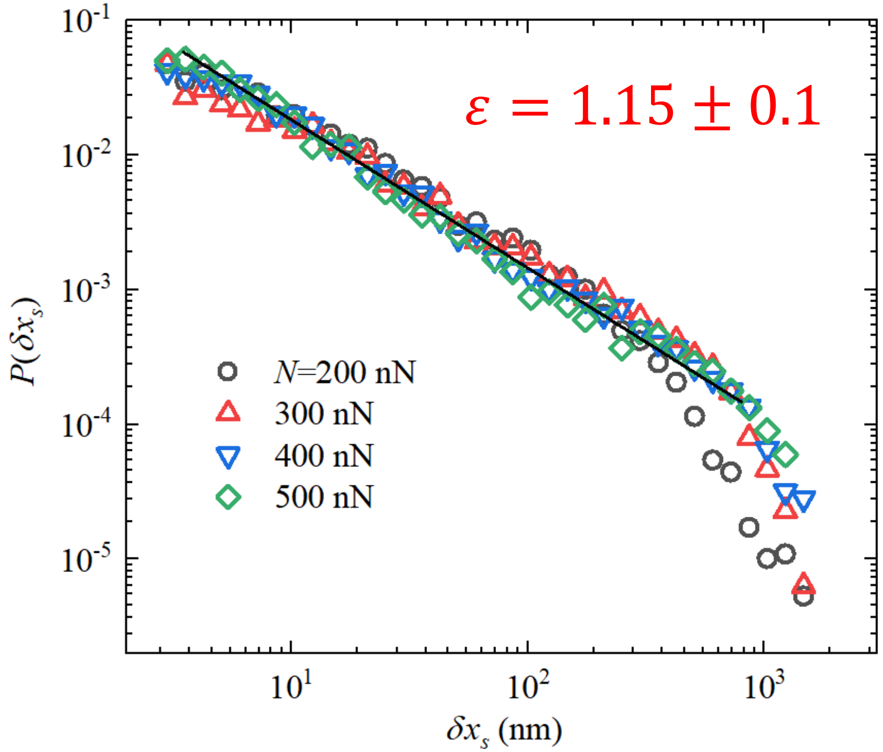

- Power-law distribution is hallmark of the avalanche dynamics.
- The power-law exponent $\varepsilon \sim 1.5$ (ABBM) of the CL is larger than that of the solid friction: $\varepsilon \sim 1.2$ (quasi-1D), $\varepsilon \sim 0.72$ (2D probe).

Distribution of the stick-slip events: Dynamic spring constant k

Contact line

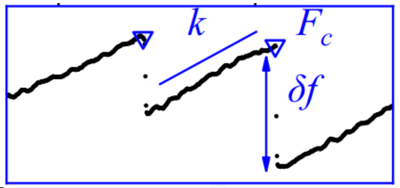

Solid friction

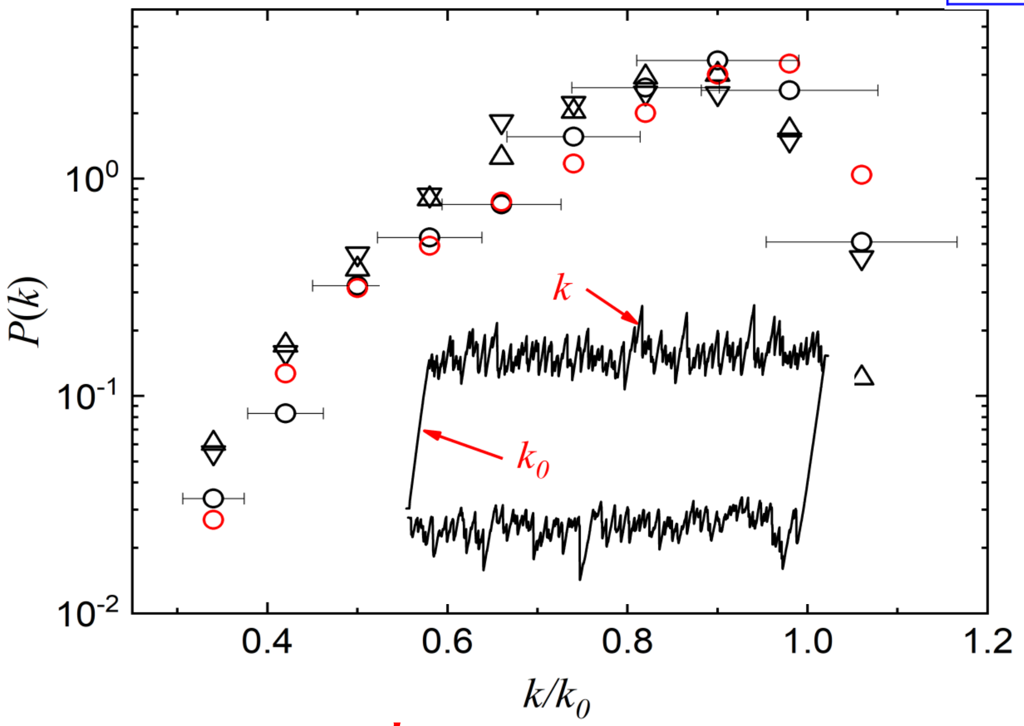

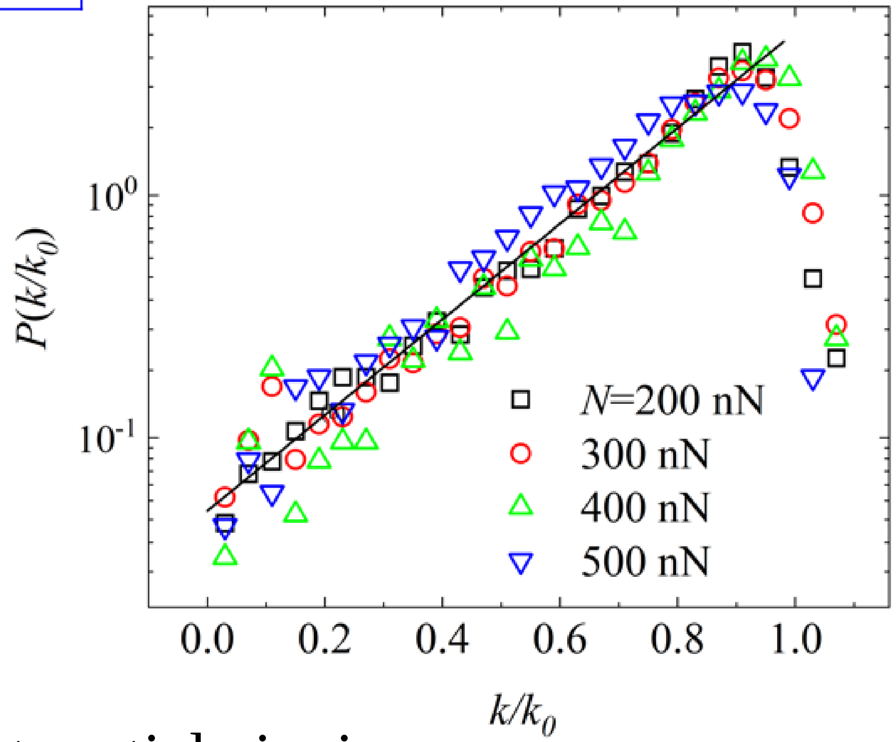

k is the dynamic spring constant at partial pinning.

k_0 is the static spring constant at complete pinning.

$0.3 \lesssim k/k_0 \lesssim 1.1$ and peaks around $k/k_0 \simeq 0.94$

→ k_0 sets a cutoff value for k

Theoretical model: Stick-slip motion in a random pinning field

$h(x; z)$: defect-induced heterogeneous interfacial tension difference between the solid-air and solid-liquid interfaces

Elastic pulling force

$$F_{pull} = k_0(z - \bar{z}_{cl}),$$

$$F_{pin} = \int_0^{\pi d} h(x; z_{cl}(x))dx.$$

Random pinning force field $F_{pin}(x)$

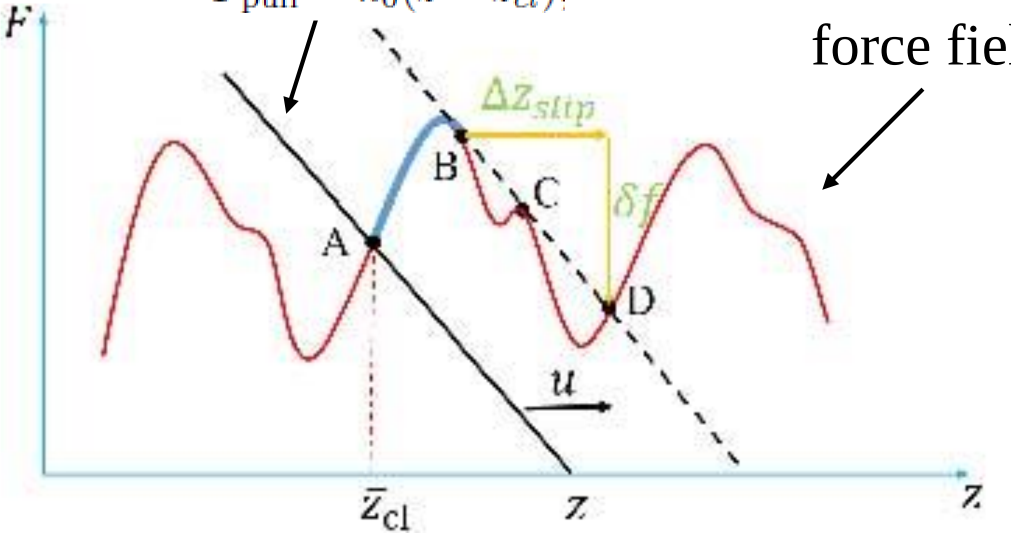

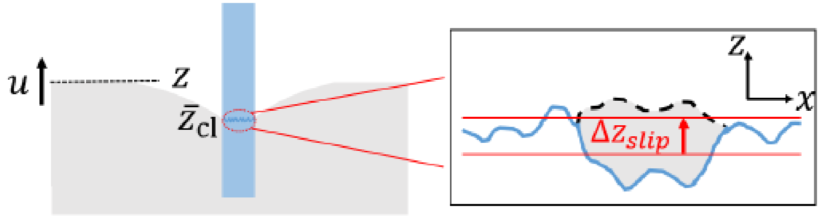

$$\bar{z}_{cl} = (1/\pi d) \int_0^{\pi d} z_{cl}(x)dx$$

Dynamic balance between F_{pull} and F_{pin}

Uphill (A→B):

Measured dynamic spring constant $k' = dF_{pin}/d\bar{z}_{cl} > 0$, is the local force gradient, with (in series)

$$\frac{1}{k} = \frac{1}{k_0} + \frac{1}{k'}$$

Downhill (B→C):

Slip instability occurs when $k_0 < k'$.

Slip length $\Delta z_{slip} = \frac{\delta f}{k_0}$.

Microscopically: $\delta f = -\langle \partial h/\partial z \rangle_A \int_A dxdz = \frac{k_0}{\pi d} \int_A dxdz = k_0 \Delta z_{slip}$

the slip area

Distribution of the stick-slip events: local pinning force gradient k'

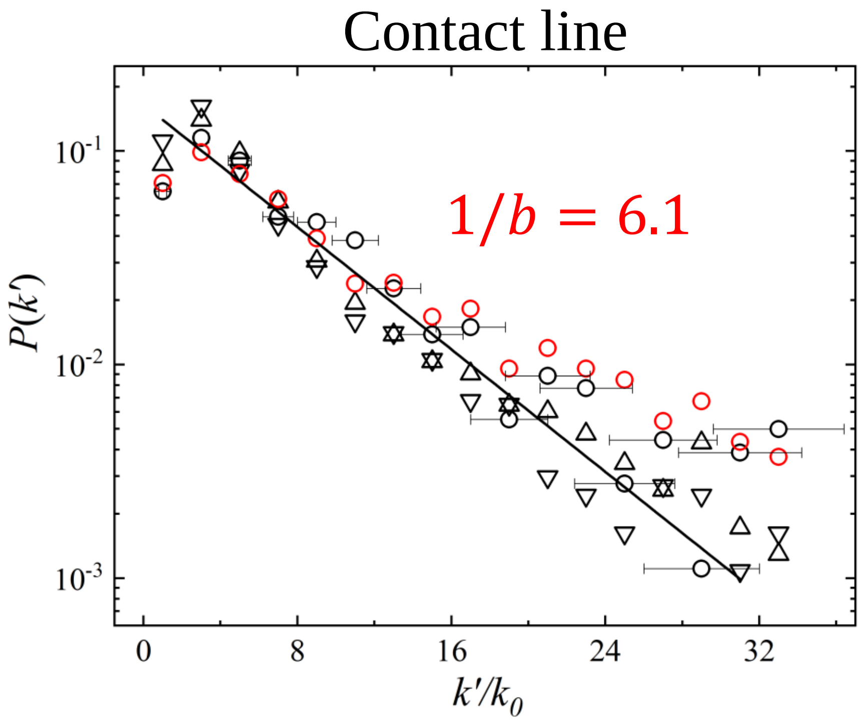

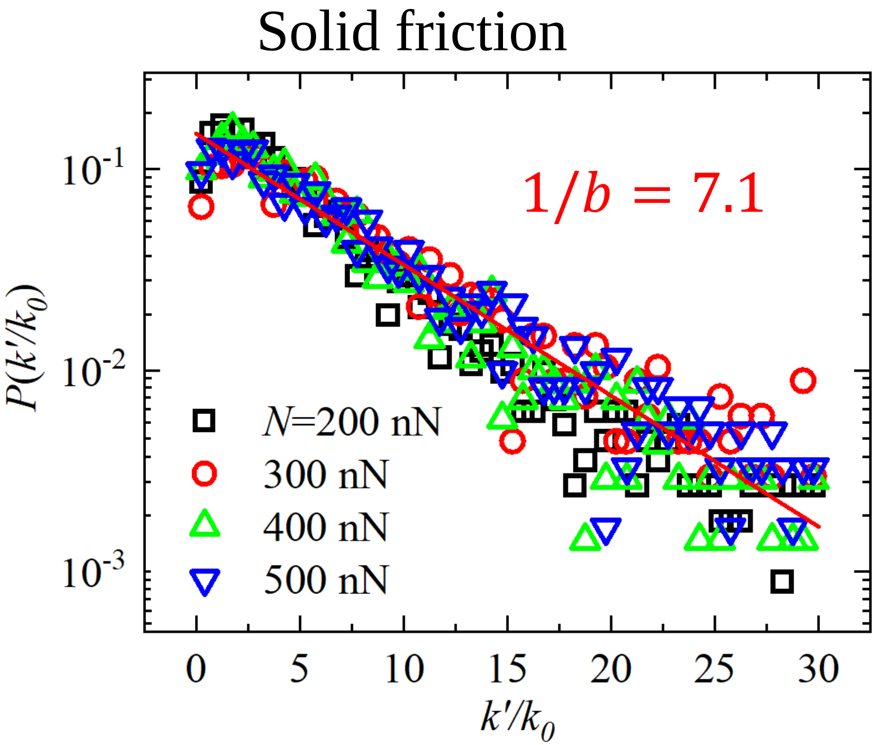

- $P(k') = \frac{1}{b}\exp[-b(k'/k_0)]$, with $\langle k'/k_0 \rangle = \frac{1}{b} \gg 1$ (stick-slip condition is satisfied).
- Exponential distribution of k' is common in dynamically or spatially heterogeneous systems
- Broad surface height roughness distribution:

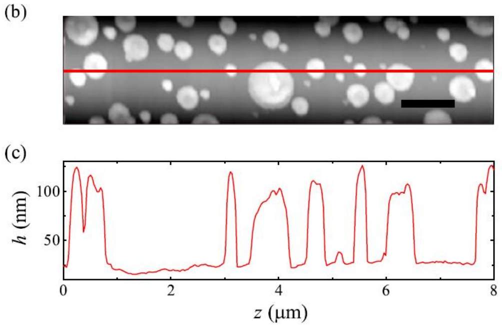

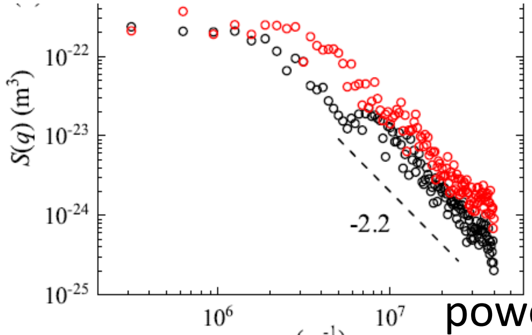

power spectrum

Damped spring-block model for stick-slip dynamics

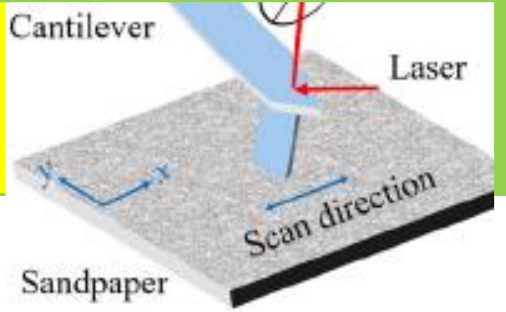

Governing equation of the stick-slip motion (center-of-mass of scanning probe x_s):

$$m\frac{d^2x_s}{dt^2} = -\gamma\frac{dx_s}{dt} + k(u_0t - x_s) - F_{\text{pin}}(x_s)$$

Brownian-correlated pinning force:

$$\langle\left|F_{\text{pin}}(x_s) - F_{\text{pin}}(x_s')\right|^2\rangle = 2D|x_s - x_s'|$$

- an extension of the Prandtl and Tomlinson model (widely used in the study of atomic stick-slip friction), in which $F_{\text{pin}}(x_s)$ was assumed to be of a sinusoidal form for atomic friction over a single crystalline surface.

$U = \frac{dx_s}{dt}/u_0$ → Langevin-type equation with multiplicative noise:

$$\alpha\frac{d^2U}{dT^2} = -\frac{dU}{dT} + 1 - U + \sqrt{U}\xi(T); \qquad \langle\xi(T)\rangle = 0, \langle\xi(T)\xi(T')\rangle = 2D'\delta(T - T')$$

$$\alpha = mk/\gamma^2\begin{cases} = 0, & \text{overdamped, ABBM} \\ \geq 1/4, & \text{underdamped}\end{cases}$$

$$D' = D/k\gamma u_0\begin{cases} \gg 1, & \text{strong pinning} \\ \leq 1, & \text{weak pinning}\end{cases}$$

Numerical solution:

$$U(T = 0) = 0; U(T = T_s) = 0$$

Slip length: $\delta x_s \equiv \int_0^{T_s} U(T)dT$

Damped spring-block model for stick-slip dynamics in solid friction

Numerical results

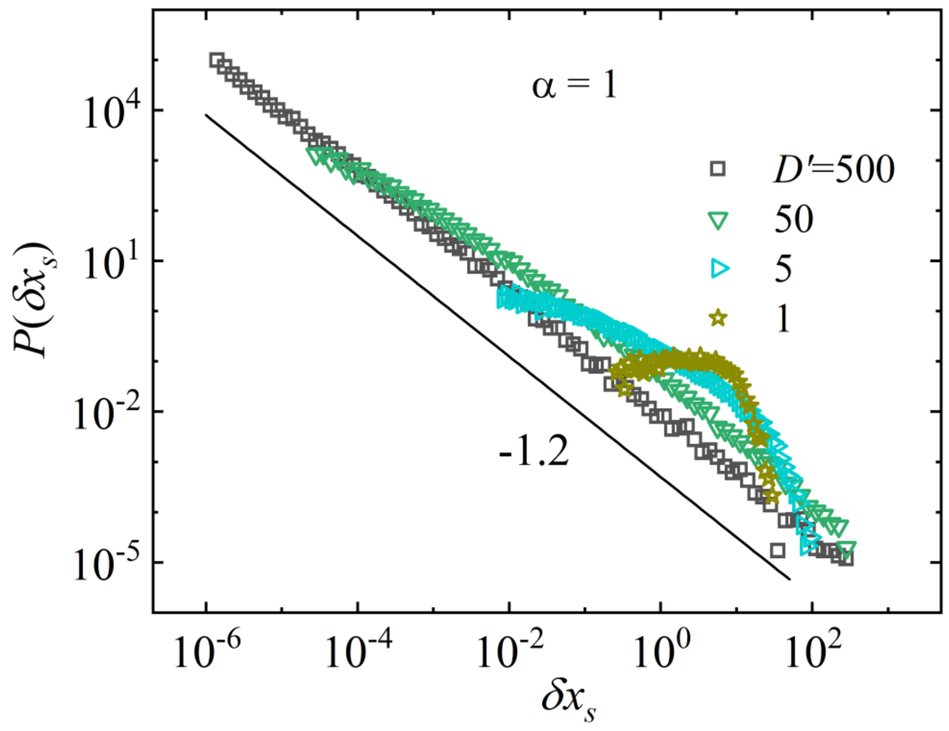

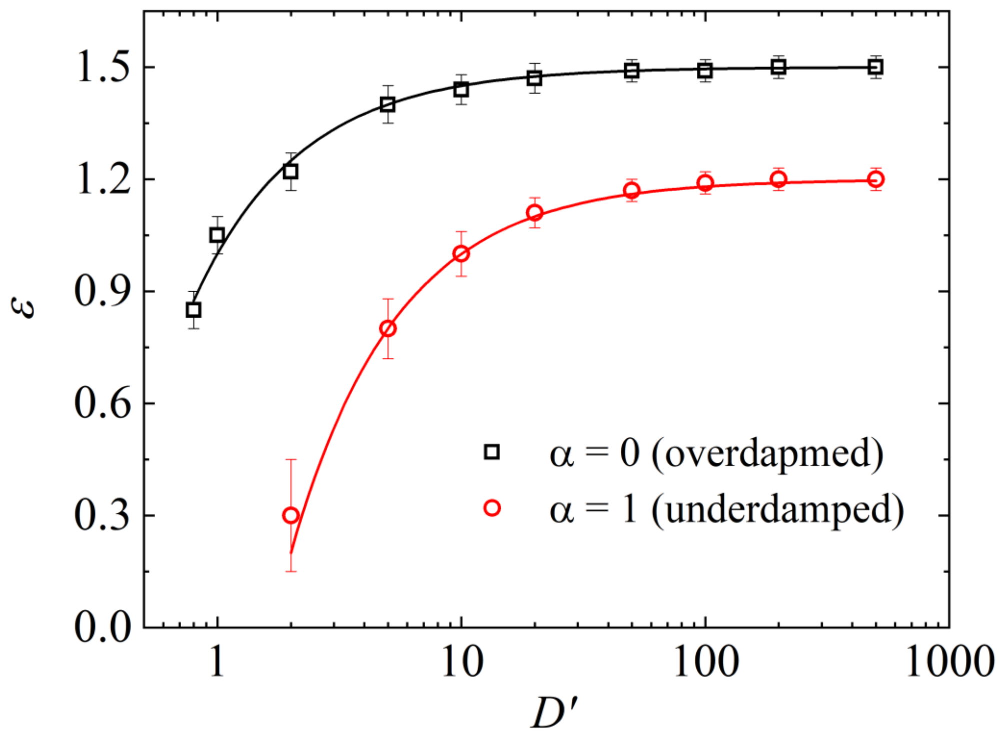

Distribution of the slip length:

$$P(\delta x_s) \sim \delta x_s^{-\varepsilon}$$

$$\epsilon = \begin{cases} 3/2 - 1/(2D'), & \alpha = 0 \text{ (overdamped, ABBM)} \\ 1.2 - 2/D', & \alpha \geq 1/4 \text{ (underdamped)} \end{cases}$$

Smaller ϵ for under-damped system: it has less dissipation, and more slip events with larger slip lengths are observed

Conclusions

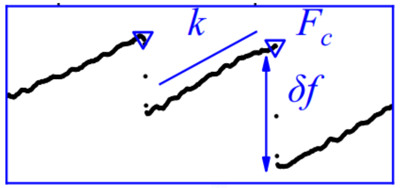

$\delta f = k_0 \delta x_s$

- Stick-slip friction and contact line pinning-depinning at mesoscale (at the single slip resolution) obey the statistical laws that are often associated with the avalanche dynamics at a critical state.
- seemingly chaotic stick-slip friction at mesoscale obeys precise statistical laws
- The avalanche (stick-slip) dynamics of a contact line or solid are governed by three statistical laws:
  1) GEV distribution for the depinning force;
  2) Power-law distribution of the slip length;
  3) Exponential distribution of the local pinning force gradient k'

$P(\delta x_s) \sim (\delta x_s)^{-\varepsilon}$

- The power-law exponent ε for the avalanche size can be caused by the magnitude of damping, with $\varepsilon = 1.5$ for the overdamped contact line and $\varepsilon \sim 1.2$ for the (quasi 1D)underdamped solid friction.
- The proposed damped spring-block model under a Brownian-correlated pinning force field captures the essential physics of the stick-slip friction at mesoscale

Collaborators:

Penger Tong (HKUST), Hsuan-Yi Chen (National Central University, Taiwan)

Dr. Caishan Yan (HKUST), Dr. Dongshi Guan, Dr. Yin Wang

- "Statistical laws of stick-slip friction at mesoscale", Nature Comm. **14**:6221 (2023).
- "Avalanches and extreme value statistics of a mesoscale moving contact line, PRL **132**, 084003 (2024) (Editor's suggestion)